© 2016. Published by The Company of Biologists Ltd | Journal of Cell Science (2016) 129, 2190-2201 doi:10.1242/jcs.184663

RESEARCH ARTICLE

Basolateral sorting and transcytosis define the Cu+-regulated translocation of ATP7B to the bile canaliculus

Vasiliki Lalioti[1], Ramón Peiró[2], Manuela Pérez-Berlanga[1], Yo Tsuchiya[1,*], Angeles Muñoz[3], Teresa Villalba[3], Carlos Sanchez[3] and Ignacio V. Sandoval[1,‡]

ABSTRACT

The Cu^+ pump ATP7B plays an irreplaceable role in the elimination of excess Cu^+ by the hepatocyte into the bile. The trafficking and site of action of ATP7B are subjects of controversy. One current proposal is that an increase in intracellular Cu^+ results in the translocation of ATP7B to the lysosomes and excretion of excess Cu^+ through lysosomal-mediated exocytosis at the bile canaliculus. Here, we show that ATP7B is transported from the trans-Golgi network (TGN) to the bile canaliculus by basolateral sorting and endocytosis, and microtubule-mediated transcytosis through the subapical compartment. Trafficking ATP7B is not incorporated into lysosomes, and addition of Cu^+ does not cause relocalization of lysosomes and the appearance of lysosome markers in the bile canaliculus. Our data reveal the pathway of the Cu^+-mediated transport of ATP7B from the TGN to the bile canaliculus and indicates that the bile canaliculus is the primary site of ATP7B action in the elimination of excess Cu^+.

KEY WORDS: Copper, ATP7B, Trafficking, TGN, Bile canaliculus, Transcytosis

INTRODUCTION

The redox properties of Cu^+ endow the metal with the simultaneous ability to be both essential and potentially damaging to the cell. Thus, as the cell only needs Cu^+ in trace amounts, to counter the relative high levels of Cu^+ in food, animals have developed sophisticated mechanisms to chaperone, store and eliminate excess Cu^+. In the liver, hepatocytes act as the major captor of the Cu^+ absorbed in the digestive tract, the main reservoir and distributor of Cu^+ to other tissues and organs, as well as the key mediator of Cu^+ elimination through excretion into bile (Harris, 2000; Lalioti et al., 2009). Because of these three functionalities, the liver plays an essential role in Cu^+ homeostasis in mammals, birds and reptiles.

In the hepatocyte, the elimination of Cu^+ is mediated by ATP7B, a membrane pump specialized for the vectorial transport of Cu^+ (Bull et al., 1993; Tanzi et al., 1993). At physiological concentrations of Cu^+, ATP7B is localized to the trans-Golgi network (TGN), where it functions in the transfer of Cu^+ to secretory proteins, such as ceruloplasmin. Increased Cu^+ levels in the hepatocyte result in the release of the ATP7B that has been sequestered in the trans-Golgi network (TGN) and its relocation to other membrane compartments. However, although the direct relocalization of ATP7B to the bile canaliculus would appear to be the most likely trafficking route, studies on the Cu^+-induced relocation of ATP7B have resulted in identification of other membrane targets, including late endosomes and lysosomes (Harada et al., 2003a; Polishchuk et al., 2014; Weiss et al., 2008). In addition, a stable pool of ATP7B has been located at tight junctions (Hernandez et al., 2008). The detection of Cu^+ within lysosomes carrying ATP7B in their membranes and the increase in trafficking of ATP7B to the bile canaliculus upon activation of lysosomal exocytosis, together with the recent report that brief exposure to Cu^+ activates lysosomal exocytosis, has led to the proposal that ATP7B pumps excess Cu^+ into lysosomes and that the lysosomes loaded with Cu^+ then fuse with the membrane of the bile canaliculus (Polishchuk et al., 2014). These observations are in contrast with studies indicating that ATP7B is transported from the Golgi to the bile canaliculus (Guo et al., 2005; Hernandez et al., 2008; Roelofsen et al., 2000) and recent evidence indicating that transport to the bile canaliculus occurs through a trans-endosomal pathway (Lalioti et al., 2014; Nyasae et al., 2014).

Although more than 300 mutations in the ATP7B gene that affect the function and cellular distribution of ATP7B have been associated with Wilson disease – a rare autosomal Cu^+ toxicosis (Kenney and Cox, 2007) – the tight association between the trafficking and function of ATP7B in Cu^+ donation and elimination makes it likely that some Cu^+ metabolism abnormalities are caused by dysfunction of membrane protein trafficking and regulation, which might also affect the distribution of other proteins. With regard to this, it is interesting that mutation of the AP1S1 gene, which codes for the σ1A subunit of the clathrin adaptor AP-1 that is involved in the intracellular trafficking of Cu^+ transporters ATP7B and ATP7A (Holloway et al., 2013; Jain et al., 2015; Lalioti et al., 2014), causes MEDNIK syndrome, which includes a disorder in Cu^+ homeostasis (Martinelli et al., 2013). Furthermore, deficiency of COMMD1, a protein component of the COMMD–CCDC22–CCDC93 (CCC) complex that plays an important role in the trafficking of retromer cargo, results in defective Cu^+ homeostasis (Phillips-Krawczak et al., 2015; van De Sluis et al., 2002).

It is thus important to characterize the trafficking pathway of ATP7B in the hepatocyte and the site of ATP7B action, not only to enable the identification of the genetic defects associated with Cu^+ toxicosis, but also to understand the presentation and course of those disorders, and to design specific strategies to prevent and treat them.

We describe here the characterization of the Cu^+-dependent pathway of ATP7B translocation from the TGN to the bile canaliculus in the polarized rat hepatoma Can 10 cell line. Our results indicate that upon Cu^+-induced release from the trans-Golgi network, ATP7B is initially sorted to the basolateral membrane and then transported by transcytosis to the bile canaliculus via a

[1]Department of Cell Biology and Immunology, Centro de Biología Molecular Severo Ochoa, Cantoblanco, Madrid 28049, Spain. [2]Department of Genomics and Massive Sequencing, Centro de Biología Molecular Severo Ochoa, Cantoblanco, Madrid 28049, Spain. [3]Department of Optical and Confocal Microscopy, Centro de Biología Molecular Severo Ochoa, Cantoblanco, Madrid 28049, Spain.
*Present address: Tohoku Women's College, Hirosaki, Aomori, Japan.

‡Author for correspondence (isandoval@cbm.csic.es)

M.P.-B., 0000-0001-8129-0107; I.V.S., 0000-0003-1485-2936

Received 10 December 2015; Accepted 28 March 2016

Journal of Cell Science

Journal of Cell Science (2016) 129, 2190-2201 doi:10.1242/jcs.184663

route that includes the subapical compartment and excludes the lysosomes.

RESULTS

Polarized hepatoma Can 10 cells use the inwards-positioned apical surface to assemble bile canaliculi of different sizes and, when growing in small islets, arrange their bodies perpendicular to the bile canaliculus and project their large basolateral surface outwards (Fig. S1A–D) (Cassio et al., 2007; Hernandez et al., 2008); this arrangement greatly facilitates monitoring the changes in the distribution of ATP7B in response to increased Cu^+ levels in the cell.

ATP7B is sorted basolaterally at the TGN by acidic vesicles

Careful titration of the Cu^+-dose–ATP7B-response in Can 10 cells showed that additions of Cu^+ of >1 μM to the cell medium caused the mobilization of the ATP7B that was retained in the TGN at low Cu^+ concentrations. To study the pathway of ATP7B translocation from the TGN to the bile canaliculus, we used 40 μM Cu^+ – a concentration that causes the fast release of ATP7B from the TGN and a trafficking rate that is suitable for monitoring the redistribution of ATP7B and for characterization of the transport pathway.

ATP7B began to leave the TGN within 5 min after addition of Cu^+, and the release was completed in 15–20 min (Fig. 1A1–C2). The acidic pH of the TGN led us to study whether an increase in the pH affects the ATP7B release. To this end, we studied the release of ATP7B from the TGN in Can 10 cells that had been preincubated for 3 h with 50 μM chloroquine, an acidotropic agent that accumulates in acidic organelles, resulting in loss of acidity and osmotic swelling. The study revealed that 15 min after the addition of Cu^+, many of the vesicles transporting ATP7B out of the Golgi remained attached to the TGN and were swollen, hence indicating that the acidity of the TGN is crucial for the release of the vesicles loaded with ATP7B (Fig. 1D1).

Because V-type H^+ ATPase inhibitors are essential for organelle acidification, and because deacidification by specific inhibitors blocks TGN to plasma membrane delivery (Yilla et al., 1993), we next studied the effect of bafilomycin A1 on the release of ATP7B from the TGN. In cells that had been treated for 3 h with 100 nM bafilomycin A1 and was then challenged for 15 and 25 min with Cu^+, we found that the drug caused the segregation of the cisterna that had the appearance of 'bunches of grapes' and was loaded with ATP7B from the cisterna hosting the TGN marker TGN38 (Fig. 1E–G) before the 'grape'-like cisterna broke into clusters of EEA1-positive-endosomes (Fig. 1H) (see Discussion). The rapid incorporation of the early endosome marker EEA1 into the vesicle clusters that originate from the Golgi had been observed in cells transfected with ATP7B mutants (Lalioti et al., 2014), and might explain the localization of ATP7B in clusters of basolateral endosomes in cells that were treated with bafilomycin A1 (Nyasae et al., 2014) (see Discussion).

Remarkably, much of the ATP7B released from the TGN in cells incubated for 5–10 min with Cu^+ was found in vesicle-like structures hoarded at the far end of the basolateral domain, opposite to the apical bile canaliculus (Fig. 2A–B2), and many of those vesicles retained the EEA1 marker (Fig. S1E–G). Next, to study the presence of ATP7B in basolateral endosomes, we incubated the cells for 12 min with Cu^+ and, for the last 8 min of the incubation, with the marker of basolateral endocytosis Alexa-Fluor-647–transferrin. The detection of transferrin in vesicles loaded with ATP7B at the far end of the basolateral domain, opposite to the bile canaliculus, was consistent with the transport of ATP7B through basolateral endosomes after its release from the TGN (Fig. 2C1–C3; Table S1).

Basolaterally sorted ATP7B is not incorporated into lysosomes

The acidity of the vesicles loaded with ATP7B that pinch-off from the TGN and the reported ability of Cu^+ to induce the direct and fast incorporation of ATP7B into late endosomes and/or lysosomes (Polishchuk et al., 2014) prompted us to examine those vesicles and the incorporation of ATP7B into lysosomes during ATP7B relocation to basolateral endosomes. To this end, and to minimize the chances that ATP7B would be incorporated into a discrete or small population of lysosomes, causing the event to pass unnoticed, we compared separately the distributions of ATP7B and four lysosomal integral membrane proteins (LIMPs) – CD63, LIMPII, LAMP1 and LAMP2 – that are unevenly distributed among late endosomes, plasma membrane, specialized phagosomes and secretory vesicles (Fig. 3A) (Barriocanal et al., 1986; Metzelaar et al., 1992). Two of these proteins, CD63 and LAMP1, have been used in the study that described the Cu^+-induced incorporation of ATP7B into lysosomes of HepG2 cells (Polishchuk et al., 2014).

The possible incorporation of ATP7B into lysosomes and of LIMPs into ATP7B vesicular carriers was next studied by comparing separately the distributions of ATP7B and the LIMPs CD63, LIMP II and LAMP2 in cells that had been treated for 15 min with Cu^+ in order to induce the bulk of ATP7B to move through the basolateral domain (Fig. 3B1–B6,C1,D1,E1). Under these conditions, the average ATP7B:LIMPs coincidence ratio in ATP7B vesicles and lysosomes was never higher than 0.0206:1 (Table S2). Furthermore, using the non-parametric Kolmogorov and Wilcoxon tests (Tables S4 and S5) to analyze the non-normal distribution of pairs of the CD63, LIMP II and LAMP1 populations (Fig. S3A, Table S3), we found that the association of ATP7B and LIMPs in ATP7B-positive vesicular carriers and lysosomes can be described by the two separate populations CD63 and LIMPII–LAMPI, with intervals of confidence of $[4.156\times10^{-3}, 8.861\times10^{-3}]/[1.315\times10^{-2}, 2.082\times10^{-2}]$ and $[3.247\times10^{-3}, 6.93\times10^{-3}]/[1.153\times10^{-2}, 1.886\times10^{-2}]$, respectively (Table S6). These intervals reaffirmed the calculated ATP7B:LIMPs coincidence ratio lower than 0.0206:1, a value that fell dramatically short of the 0.40:1 ratio reported in HepG2 cells (Polishchuk et al., 2014). Altogether, these data indicate that the vesicles that transport ATP7B through the basolateral domain are structures that are distinct from lysosomes.

ATP7B is inserted into the basolateral membrane and endocytosed

To identify whether the presence of ATP7B in basolateral endosomes resulted from the fusion of endosomes with the vesicles that transported ATP7B to the basolateral domain, or from the ATP7B insertion into the basolateral membrane and subsequent endocytosis, we studied the effect of dynasore (DYN), the inhibitor of dynamin and clathrin-dependent endocytosis. We repeated the transferrin-loading experiment in cells that had been transfected with exofacial hemagglutinin (HA)-tagged ATP7B, followed by simultaneous incubation of the cells with Alexa-Fluor-647–transferrin and an antibody against HA. Treatment of cells for 60 min with DYN before challenge with Cu^+ showed a marked retention of ATP7B in the basolateral surface and a complete inhibition of its incorporation into the bile canaliculi, an effect that was strongly reversed after washing out the drug (compare Fig. 4A1–A3 and 4B1–B3). Moreover, in cells that had been transfected with HA–ATP7B, we located the endocytosed HA tag and Alexa-Fluor-647–transferrin in endosomes transporting ATP7B

Journal of Cell Science (2016) 129, 2190-2201 doi:10.1242/jcs.184663

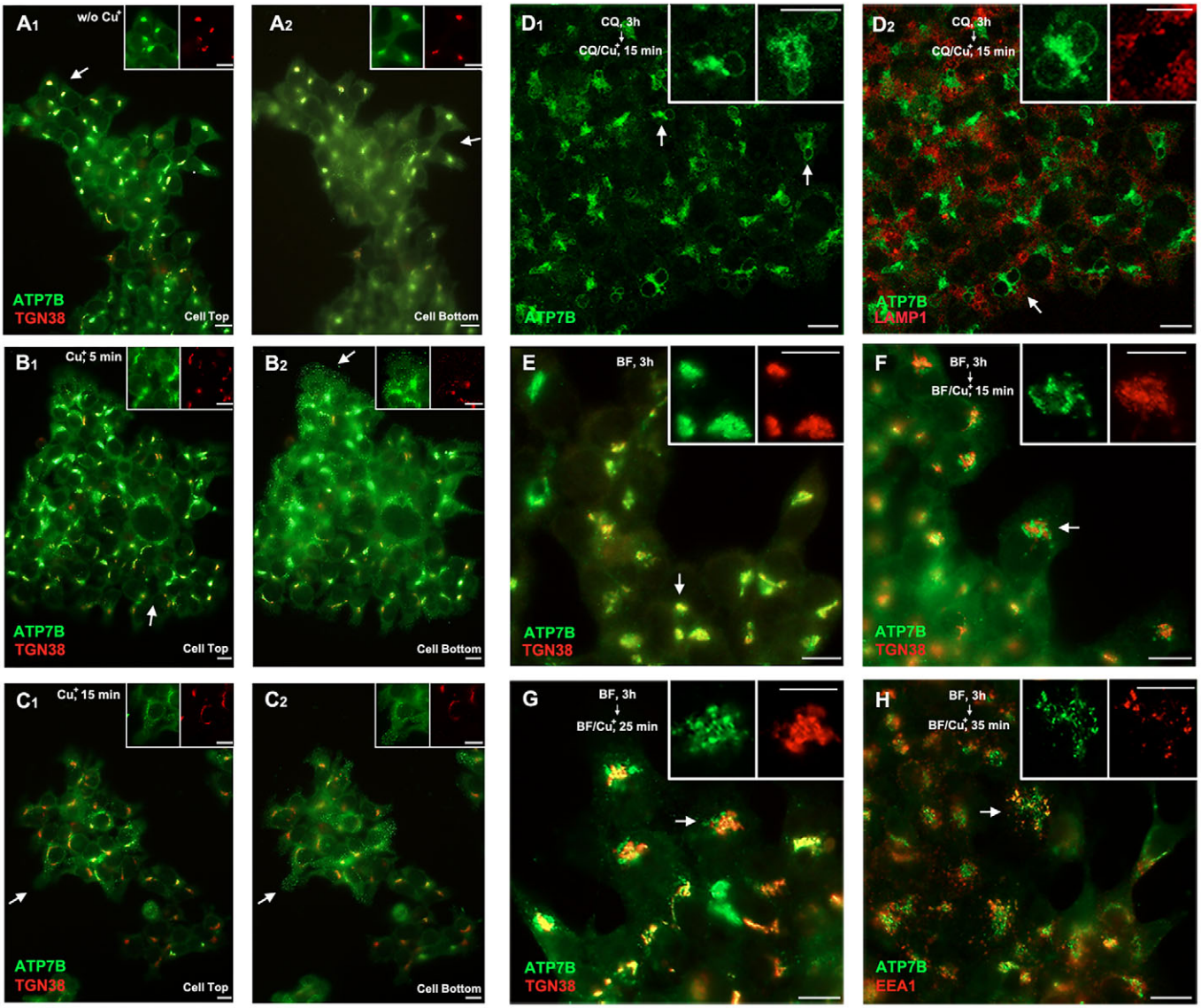

Fig. 1. ATP7B is quickly released from the TGN in response to Cu^+. Can 10 cells were treated with 40 µM Cu^+ for the indicated times and immunostained for ATP7B and the TGN marker TGN38 (A1–C2); w/o, untreated controls. ATP7B is transported out of the TGN by acidic vesicles: chloroquine (CQ) induces swelling and retards the release of ATP7B-loaded vesicles emerging from the TGN upon Cu^+ stimulation. Can 10 cells that had been treated for 3 h with 50 µM chloroquine followed by 15 min with 40 µM Cu^+ + cloroquine were stained for ATP7B and the lysosomal integral membrane protein LAMP1. Confocal microscopy of a 0.04-µm optical section was then performed (D1,D2). The intense fluorescence produced by the ATP7B was retained in the vesiculated TGN and in swollen vesicles attached to the TGN that are distinct from the lysosomes. Inhibition of the V-H^+ pump slows down the packing of ATP7B at the TGN into transport vesicles. Cells that had been treated for 3 h with 100 nM bafilomycin A1 and then with 40 µM Cu^+ and the drug for the times indicated were stained for ATP7B, TGN38 and EEA1, and studied by performing microscopy (E–H). Note, the 'bunch of grapes' appearance of the cisternae loaded with ATP7B and that the physical segregation of these cisternae replicates that of the TGN38-positive cisternae (F,G), before breaking down into vesicles that acquire the early endosome marker EEA1 (H). Areas indicated with arrows are enlarged in the insets in separate color channels. Scale bars: 10 µm. BF, bafilomycin A1.

(Fig. 4C1–C3). These two studies strongly indicate that, after its release from the TGN, ATP7B is targeted to the basolateral domain and inserted into the basolateral membrane, and is then endocytosed.

To investigate whether ATP7B interacts with AP-2, the clathrin adaptor complex that participates in clathrin-mediated endocytosis of cargo, we examined the ability of ATP7B and the α subunit of the AP-2 adaptor to pull each other down in inmunoprecipitation assays (Fig. 4D). Confirmation of this ability indicates that the surface-localized AP-2 might participate in the clathrin-mediated endocytosis of ATP7B that is inhibited with DYN.

ATP7B is vectorially transported from the basolateral to the apical domain by a mechanism that requires microtubules

To examine the redistribution of the basolateral endosomes loaded with ATP7B and transferrin, we extended the treatment of cells with Cu^+ to 25 min and postponed the addition of transferrin to the last 10 min of incubation with Cu^+ (Fig. 2D1–D3). Under these conditions, ATP7B began to appear in the apical pole of the cells and to dissociate from basolateral endosomes loaded with transferrin (compare Fig. 2C and 2D; Table S1). It is well established that vesicle-mediated transcytosis from the basolateral to the apical domain requires microtubules (Hunziker et al., 1990). To explore whether transport of ATP7B to the apical pole requires

Journal of Cell Science

Journal of Cell Science (2016) 129, 2190-2201 doi:10.1242/jcs.184663

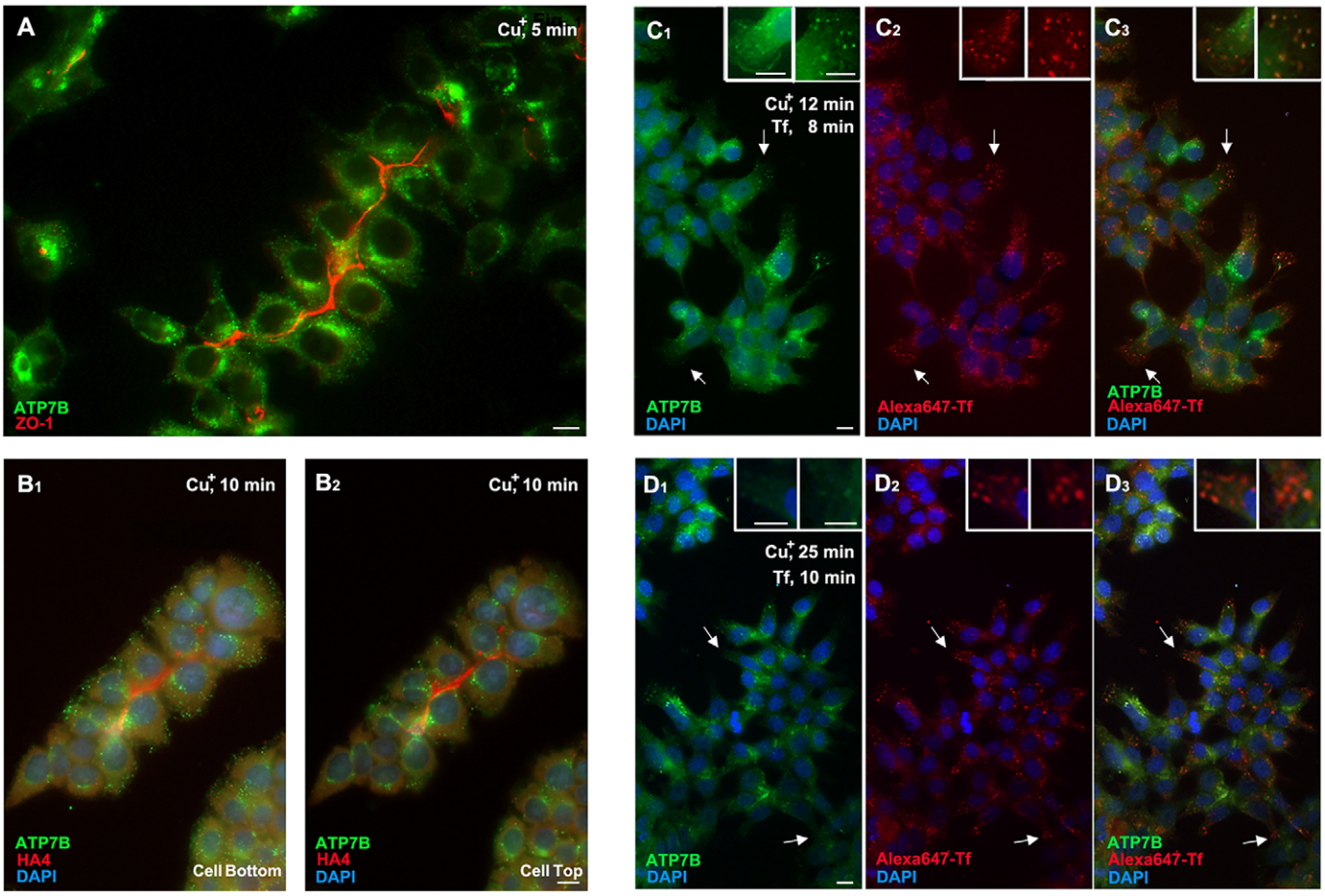

Fig. 2. ATP7B-loaded vesicles are rapidly relocated to the cell basolateral domain after their release from the TGN. Can 10 cells that had been treated with 40 µM Cu^+ for the times indicated were stained for ATP7B (A,B1,B2), the tight junction marker ZO-1 (A) or the marker of the bile canaliculus membrane, HA4 [B1,B2]; nuclei were stained with DAPI. Localization of ATP7B in basolateral endosomes loaded with endocytosed transferrin. Cells were treated for 12 min with Cu^+ and with Alexa-Fluor-647–transferrin (Tf) for the last 8 min (C1-C3), or for 25 min with Cu^+ and with Alexa-Fluor-647–transferrin for the last 10 min (D1–D3). Arrows indicate areas enlarged in the insets. Treated cells showed the loading of basolateral endosomes with ATP7B and endocytosed transferrin. Scale bars: 10 µm.

microtubules, we incubated Can 10 cells for 15 min with Cu^+, to target the ATP7B retained in the TGN to the basolateral domain, and then for 60 min at 4°C with the microtubule inhibitor nocodazole (NOC) before incubation for 40 min at 37°C with or without NOC and with Alexa-Fluor-647–transferrin, in the continuous presence of Cu^+ (Fig. 5). The results showed that in cells warmed in NOC, and therefore without microtubules, the translocation of ATP7B to the apical domain was strongly inhibited and the protein was retained in numerous vesicles dispersed throughout the cytoplasm, many of them loaded with transferrin (Fig. 5B1–B5). In contrast, the washing out of NOC immediately before warming of the cells resulted in complete reconstruction of the microtubule network and in translocation of ATP7B to the apical bile canaliculus (Fig. 5C1–C5).

ATP7B enters the subapical compartment, and brefeldin A blocks the targeting of ATP7B from the subapical compartment to the bile canaliculus

Accumulation of ATP7B in the cell apical pole, where the subapical compartment (SAC) operates as a protein sorting hub (Hoekstra et al., 2004), occurred within the 15–30-min window after the addition of Cu^+ (Fig. 6A1–A3). This movement was preceded by the segregation of the ATP7B and transferrin loads (Fig. S2A1–A3), with transferrin being targeted to the area adjacent to the nucleus, where clusters of common recycling endosomes recover transferrin back to the basolateral surface.

Examination of the ATP7B distribution in the apical pole showed a high degree of coincidence between ATP7B and Rab11a, the small GTPase associated with the SAC that regulates the apical transport and recycling of proteins (Welz et al., 2014) (Fig. 6A1–A3,B). Furthermore, microscopy studies provided evidence of the transient co-distribution between the two proteins, consistent with the passage of ATP7B through the Rab11a-positive SAC before its incorporation into the bile canaliculus (Fig. 6C1–F3). Separate study of the association of CD63, LIMPII and LAMP1 with the ATP7B transiting through the SAC in cells that had been incubated for 25 min with 40 µM Cu^+ showed no evidence of association (Fig. 3C2,D2,E2; statistics are given in Table S7), and analysis of the experimental data using a geometric distribution that allows the estimation of the probability to detect one LIMP signal in the SAC produced a value of $p_{SAC}<0.049$ ($\bar{p}_{SAC} = 0.033$) at a 95% confidence level that strongly endorsed the experimental observations (Fig. S3B, Table S7).

Transport of ATP7B from the apical pole to the bile canaliculus is inhibited by the ARF-GEF inhibitor brefeldin A

The fungal toxin brefeldin A (BFA) specifically targets the large ARFs, GTPases that regulate trafficking pathways by recruiting the

Journal of Cell Science (2016) 129, 2190-2201 doi:10.1242/jcs.184663

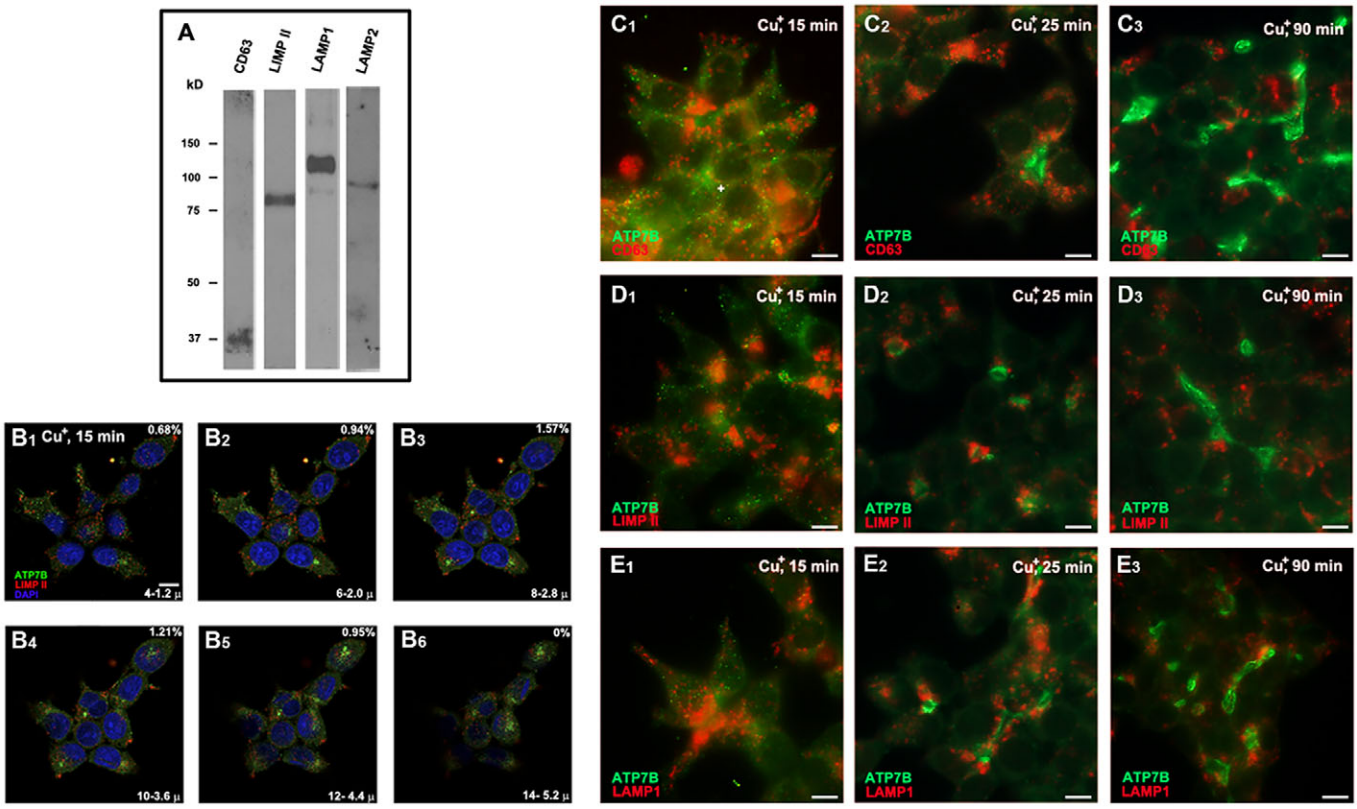

Fig. 3. ATP7B is not incorporated into lysosomes during trafficking through the somatobasolateral domain of Can 10 cells. Reactivity of mouse monoclonal antibodies with CD63, LIMP II and LAMP1 in Can 10 cells extracts and of rabbit polyclonal antibody with LAMP2 (A). Optical sections from Can 10 cells incubated for 15 min with 40 µM Cu^+ and stained for ATP7B and LIMP II are shown in B1–B6; top right, percentage of lysosomes containing ATP7B; bottom right, optical section number and distance to the plane of cell attachment; nuclei were stained with DAPI. Can 10 cells were incubated for 15, 25 and 90 min with 40 µM Cu^+ to compare the cellular distributions of ATP7B and the lysosomal membrane markers CD63, LIMP II and LAMP1 during ATP7B trafficking through the basolateral domain (C1,D1,E1) and the SAC (C2,D2,E2), and after its incorporation into the bile canaliculus (C3,D3,E3). Scale bars: 10 µm.

vesicle coat components AP clathrin adaptors, COPI and GGA proteins (Cox et al., 2004). Consistent with the localization of large GEFs in the TGN (BIG1 and BIG2, also known as ARFGEF1 and ARFGEF2) and in endosomes (BIG2), BFA caused the translocation of ATP7B from the TGN to the apical pole of HepG2 cells (Roelofsen et al., 2000) and created a characteristic patchy distribution of ATP7B that flanked the bile canaliculi in Can 10 cells (Fig. S2B1–C3). To study whether the inhibition affected the translocation of ATP7B from the apical SAC area to the bile canaliculus, we treated Can 10 cells for 15 min with Cu^+ to release the protein from the TGN, and then for 1 h at 4°C with BFA and NOC in the presence of Cu^+ before raising the temperature to 37°C and continuing the incubation with the two drugs, with BFA alone or without drugs (Fig. 6). The results showed that in cells incubated with NOC and BFA, the ATP7B protein was retained in vesicles distributed throughout the cytoplasm (Fig. 6G1–G4), whereas the removal of NOC allowed the advance of ATP7B to the apical area and its retention in SAC (Fig. 6H1–H4). Moreover, removal of NOC and BFA resulted in incorporation of ATP7B into the bile canaliculus (Fig. 6I1–I4). We therefore conclude that BFA inhibits the transport of ATP7B from the SAC to the bile canaliculus, probably by inhibiting apical BIG2. Our results were similar to those described for the transcytosis of the polymeric immunoglobulin receptor in polarized neurons, where BFA inhibits the redistribution of the receptor from the basal dendritic domain to the apical axonal domain (de Hoop et al., 1995). The relocation of the ATP7B released from the TGN culminated after its arrival at and incorporation into the bile canaliculus, as shown by its overlap with the marker of the bile canaliculus membrane HA4 (Fig. 7A1–B3). The whole translocation process required approximately 60 min (Fig. 7C). Importantly, we never observed any apically oriented movement of lysosomes during the Cu^+-dependent ATP7B translocation to the bile canaliculus. Moreover, in three separate studies of the association of CD63, LIMPII and LAMP1 with the bile canaliculus of cells that had been incubated for 90 min with 40 µM Cu^+, we did not detect any presence of LIMPs in the bile canaliculus (Fig. 3C3,D3,E3). Analysis of the experimental data using a geometric distribution produced $p_{BC}<0.019$ ($\bar{p}_{BC} = 0.013$) at a 95% confidence level, values that strongly validated the experimental observations (Fig. S3B and Table S7). With regard to this, it is significant that we never found a significant incorporation of ATP7B into the lysosomes and of lysosomal markers into the bile canaliculus of Can 10 or HepG2 cells that had been incubated under stringent Cu^+ conditions (200 µM Cu^+ for 24 h) (Fig. S4).

Apical endocytosis and recycling of ATP7B is inhibited by DYN and BFA, respectively

Treatment of cells with the non-permeable Cu^+ chelating agent bathocuproine disulphonate (BCS) induced only a slow return of ATP7B from the bile canaliculus to the TGN, probably owing to the requirement of functional ATP7B in the bile canaliculus to feed extracellular BCS with excreted Cu^+ (Fig. 7D). In contrast, the use of the cell-permeable Cu^+ chelating agent neocuproine (NEC) to

Journal of Cell Science (2016) 129, 2190-2201 doi:10.1242/jcs.184663

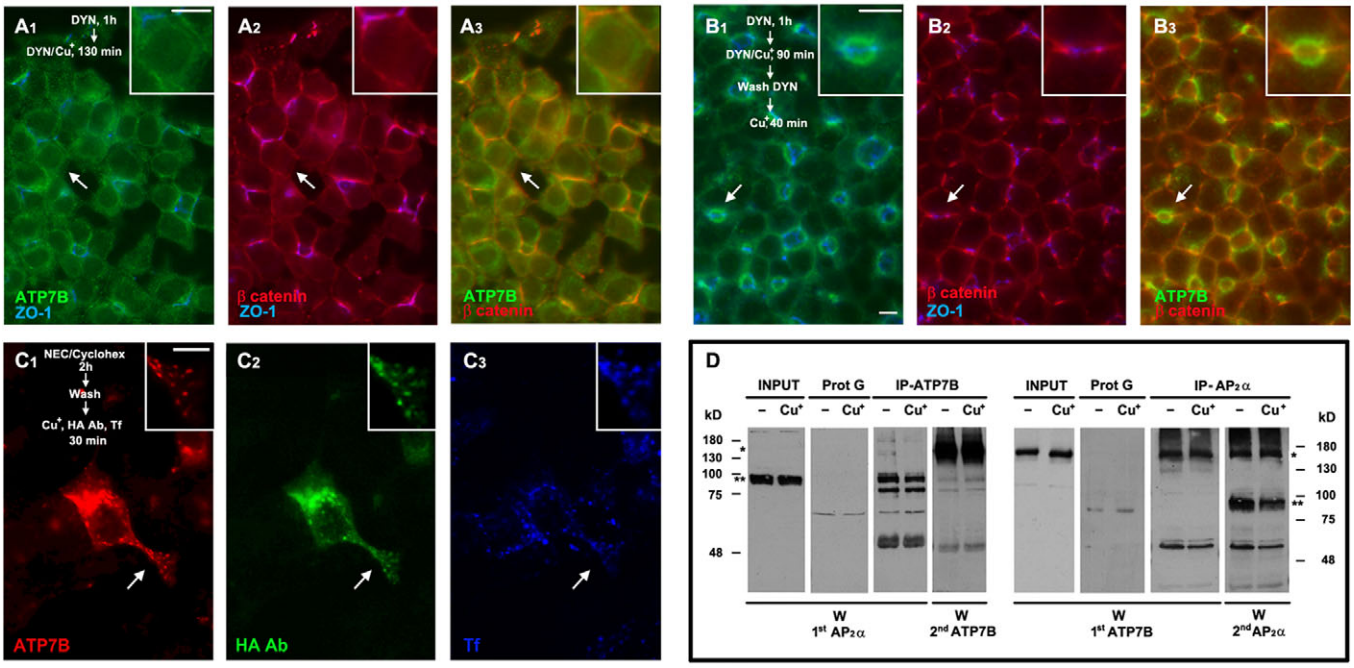

Fig. 4. Basolaterally sorted ATP7B is inserted into the basolateral membrane. DYN blocks transport of ATP7B to the bile canaliculus at the basolateral membrane. Cells that had been preincubated for 120 min with 100 µM NEC, to confine ATP7B to the TGN, were washed and treated for 60 min with 80 µM DYN and then for 90 min with 40 µM Cu^+, in the continuous presence of DYN (A1–A3) or in the absence of DYN for the last 40 min of incubation with Cu^+ (B1–B3). After fixation and permeabilization, the cells were stained for ATP7B, ZO-1 and the basolateral membrane marker β-catenin. Note the accumulation of ATP7B in the β-catenin-positive basolateral membrane of the cells that had been continuously treated with DYN, and its partial release and arrival to the bile canaliculus after DYN removal. Transfected HA–ATP7B was inserted into the basolateral membrane and endocytosed (C1–C3). Cells that had been transfected for 11 h with exofacial-HA-tagged ATP7B were incubated for 3 h in complete Coon's medium with 50 µg/ml cycloheximide (cyclohex) to inhibit new ATP7B synthesis and for the last 2 h with 100 µM NEC to retain the bulk of ATP7B in the TGN. The cells were then washed and incubated for 30 min with 100 µM Cu^+ and with 2.5 µg/ml Alexa-Fluor-647–transferrin (Tf) and 5 µg/ml of monoclonal anti-HA antibody (HA Ab). The fixed and permeabilized cells were studied by performing immunofluorescence with specific antibodies to the HA tag and ATP7B. Magnifications of ATP7B, endocytosed Alexa-Fluor-647–transferrin (false blue) and anti-HA antibody are shown in the insets. Magnified areas are indicated with arrows. Scale bars: 10 µM. (D) Pulldown of ATP7B and the clathrin adaptor AP-2α subunit (αAP2). Detergent-solubilized postnuclear supernatants from Can 10 cells that had been incubated for 15 min with or without 40 µM Cu^+ were incubated with specific antibodies to either ATP7B or the α-subunit of the AP-2 clathrin adaptor directly bound to Protein-G–Sepharose (Prot G). The immunoprecipitates were subjected to western blot analyses (W) using antibodies against the pulled down proteins. Controls included analysis of the total cell extracts (INPUT) and material precipitated by Protein-G–Sepharose alone (Prot G). The results show the reciprocal immunoprecipitation of ATP7B (*) and the AP-2 α-subunit (**) and the amounts of the AP-2α subunit pulled down by the ATP7B antibody from extracts of cells incubated in the absence or presence of Cu^+. IP, immunoprecipitation.

directly reduce intracellular Cu^+ produced a more rapid transit and, after a 2-h incubation with the drug, the bulk of ATP7B was returned to the TGN (Fig. 7D; compare Fig. 7E1–E4 and 7F1–F4). In the experiments using NEC, we observed that DYN strongly inhibited the exit of ATP7B from the bile canaliculus, indicating that the ATP7B was endocytosed by clathrin-coated vesicles (compare Fig. 7F1–F4 and 7H1–H4). In addition, we also observed that although organelle de-acidification, induced by bafilomycin A1, did not inhibit the apical endocytosis of ATP7B, it did inhibit its apical recycling and return to the TGN, retaining it in large vesicular bodies that were abundant in the subapical area adjacent to the bile canaliculus (Fig. 8A1–C4). Because the treatment with BFA inhibited the targeting of ATP7B to the bile canaliculus (Fig. 6H1–H4), we studied the possibility that the SAC is involved in the apical recycling of ATP7B by examining the distribution of ATP7B in cells that had first been treated with Cu^+ for 90 min and then incubated for a further 45 min after the addition of BFA. The incubation with BFA induced the partial re-localization of ATP7B from the bile canaliculus to the Rab11a-positive SAC (compare Fig. 7A1–B3 and 7I1–J3), resulting in the same patchy peri-canalicular distribution of the apically bound ATP7B observed in the SAC of cells treated with BFA (compare Fig. 7I1–J3 with Fig. 6H1–H4 and Fig. S2B1–C3). These results demonstrate that in cells with elevated levels of Cu^+, the ATP7B transported from the TGN to the bile canaliculus membrane was continuously endocytosed and cycled between the SAC and the bile canaliculus.

DISCUSSION

In this study, we have characterized the pathway of ATP7B transport from the TGN to the bile canaliculus in response to the elevation of intracellular Cu^+ levels in the rat hepatoma cell line Can 10.

The Cu^+-induced release of ATP7B from the TGN was found to be a rapid process that begins within 5 min of the addition of 40 µM Cu^+ and is completed within 20–25 min. Treatment with bafilomycin A1 delayed the detachment of the cisterna carrying ATP7B from the TGN, demonstrating that cisterna detachment is a prerequisite to the generation of transport vesicles, as has previously been described in plants (Uemura et al., 2014). This process is pH dependent, and the rapidity of this occurrence in mammalian cells is probably why it has not been previously observed in organisms other than plants. Our studies also show that the vesicles loaded with ATP7B budding from the TGN do not contain lysosomal membrane proteins, suggesting that these are instead segregated into vesicles distinct from those transporting ATP7B. The ATP7B carriers are then rapidly transported to a subcellular location in the large

Journal of Cell Science (2016) 129, 2190-2201 doi:10.1242/jcs.184663

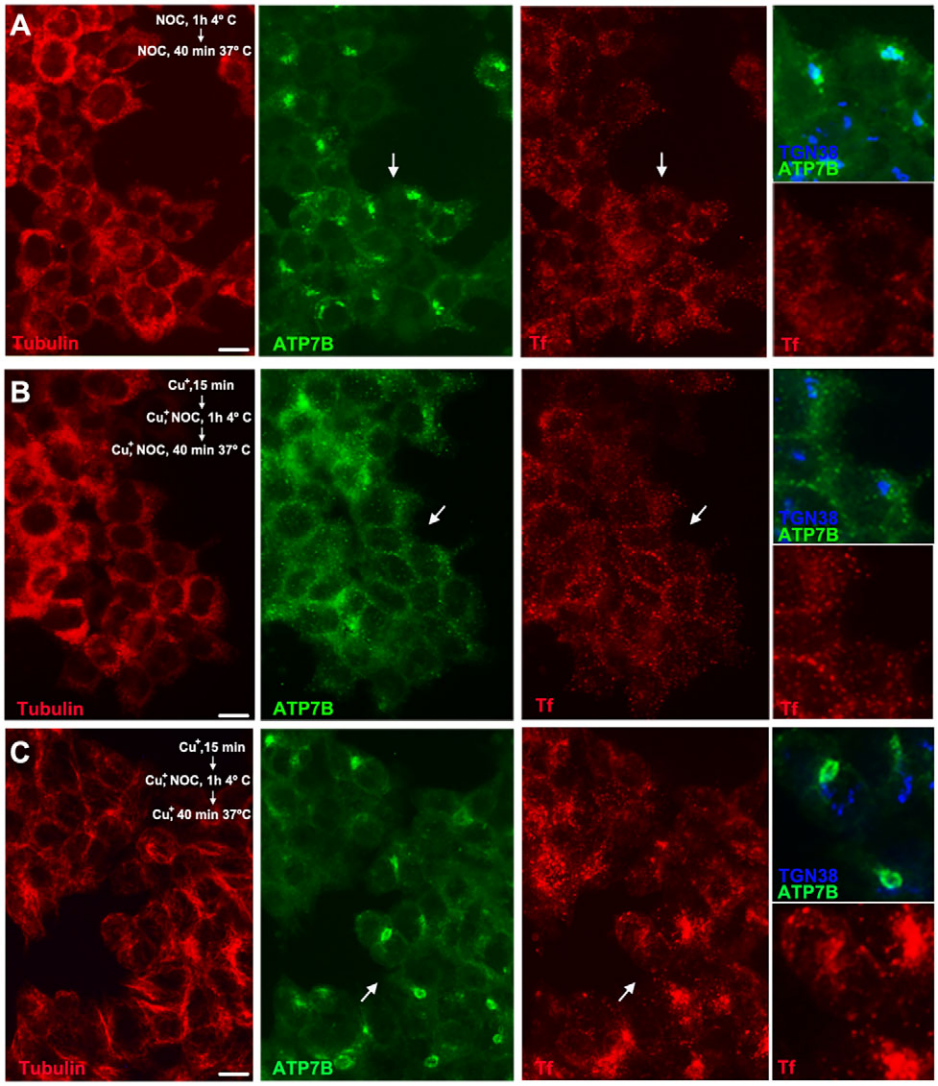

Fig. 5. ATP7B transcytosis requires microtubules. Can 10 cells were incubated for 60 min at 4°C with 20 µM NOC and then for 40 min at 37°C with both NOC and Alexa-Fluor-647–transferrin (Tf) (A1–A3), or incubated for 15 min with 40 µM Cu^{+}, to release the ATP7B retained in the TGN, followed by incubation with NOC and Alexa-Fluor-647–transferrin in the presence of Cu^{+} (B1–B3). Microtubules were reconstituted by washing out the NOC and performing the last incubation with Cu^{+} and Alexa-Fluor-647–transferrin in the absence of the drug (C1–C3). All cells were stained for ATP7B, TGN38 and microtubules (tubulin). Panels on the right-hand side (A4, A5, B4, B5, C4, C5) show magnifications of the areas indicated with arrows. Scale bars: 10 µm. Notice the retention of ATP7B in vesicles after its release from the Golgi and the disruption of microtubules, and the resumption of the ATP7B transport to the apical bile canaliculus after reassembly of microtubules.

basolateral domains of Can 10 cells, directly opposite the apical domains where the bile canaliculi are located. The basolateral sorting of ATP7B at the TGN can be explained by the Cu^{+}-mediated interaction of the C-terminal sequence motif DKWSLLL with the clathrin adaptor AP-1A complex that is resident in the TGN (Lalioti et al., 2014) because this adaptor operates in the basolateral sorting of membrane proteins in hepatocytes that lack AP-1B (Gravotta et al., 2012). The role of AP-1A in the basolateral sorting and recovery of ATP7B from endosomes to the TGN (Braiterman et al., 2011) explains why mutations in σ1A, the small subunit of the AP-1 adaptors, produce severe perturbations of copper ion metabolism in humans (Martinelli et al., 2013).

Our detection of basolaterally endocytosed transferrin in the ATP7B vesicular carriers that were localized at the distal end of the basolateral domain suggests that ATP7B is transported by basolateral endosomes and/or endocytic vesicles. This suggestion is supported by recent studies demonstrating that de-acidification of the luminal pH results in the trapping of ATP7B in aggregates of EEA1-positive endosomes that are localized to the basolateral domain of polarized WIF-B cells (Nyasae et al., 2014). Furthermore, the colocalization of both endocytosed anti-HA antibody and Alexa-Fluor-647–transferrin in the basolateral endosomes of cells that had been transfected with HA-tagged ATP7B and incubated for 30 min with Cu^{+} indicates that basolaterally sorted HA–ATP7B is first inserted into the basolateral membrane and is then subsequently endocytosed. This notion is supported by the observed accumulation of ATP7B in the basolateral membrane of cells that had been treated with DYN, an inhibitor of both dynamin and clathrin-mediated endocytosis, and the concomitant reduction in the incorporation of the ATP7B into the bile canaliculus, and is consistent with the mutual pulldown of ATP7B and the α-subunit of the clathrin adaptor AP-2, which is implicated in endocytosis. With respect to the movement of ATP7B from the basolateral to the apical domain, it is interesting that ATP7B contains an FAFDNVGYE signal motif, a variant of the [FY]XNPX[YF] signal that is recognized by the basolateral retromer and absent in ATP7A (Donoso et al., 2009), which is essential for the apical targeting of ATP7B in elevated-Cu^{+} conditions and mediates the retention of the transporter in the TGN at low-Cu^{+} concentrations (Braiterman et al., 2009).

The accumulation of ATP7B in the SAC of cells that had been incubated with BFA following endocytosis of the protein from the basolateral membrane, together with its incorporation into the bile canaliculus after removal of the drug, implicate the involvement of a large ARF-GEF that is localized in recycling endosomes, such as BIG2, in the targeting of ATP7B from the SAC to the bile canaliculus. Our finding that BFA inhibits the recycling of apically endocytosed ATP7B to the bile canaliculus by retaining the protein

Journal of Cell Science (2016) 129, 2190-2201 doi:10.1242/jcs.184663

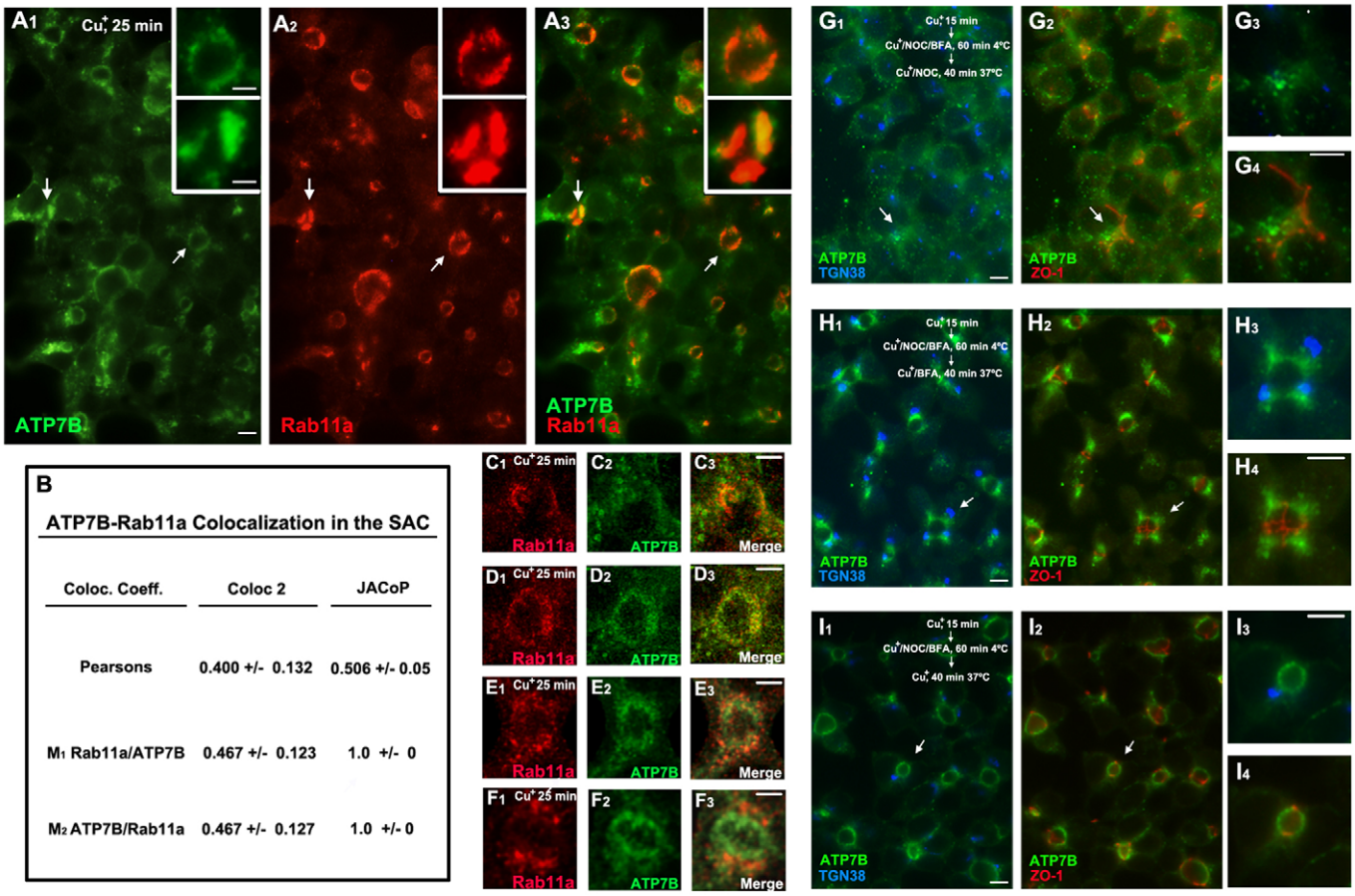

Fig. 6. Apically bound ATP7B transits through the SAC compartment. Can 10 cells were treated for 25 min with 40 µM Cu^+ and stained for ATP7B and for the SAC marker Rab11a (A1–A3); notice the characteristic two- and three-leaved arrangement of the SACs, SACs indicated with arrows are magnified in the insets. Scale bars: 10 µm. Pearson's and Manders' co-distribution coefficients (co-distribution tends to 1; median±$S_{w0.2}$) were computed using 17 confocal SAC images, and the Fiji Coloc 2 and JACoP software (B); observe the high degree of ATP7B and Rab11a co-distribution. Passage of ATP7B through the SAC was studied in cells that had been incubated for 25 min with 40 µM Cu^+ to record the ATP7B approach (C1–C3) and entrance into the SAC (D1–D3), and its subsequent incorporation into the inner circular bile canaliculus (E1–F3). Note the different rates of ATP7B entry in the SAC. Scale bars: 5 µm (C1–F3). Transport of ATP7B from the SAC to the bile canaliculus is inhibited by BFA. Can 10 cells were incubated for 15 min with 40 µM Cu^+ and then for 60 min at 4°C after the addition of 10 µg/ml BFA and 20 µg/ml NOC, before removal of BFA (G1–G4), NOC (H1–H4) or BFA and NOC (I1-I4), which was followed by incubation for 40 min with Cu^+ at 37°C. Cells were stained for ATP7B, ZO-1 and TGN38 as indicated. Panels on the right-hand side (G3, G4, H3, H4, I3, I4) show magnifications of the areas indicated with arrows. Scale bars: 10 µm. Notice the resumption of transport of the apically bound ATP7B after removal of NOC and the retention of ATP7B in the SAC of cells incubated with BFA (see also Fig. S2), as well as the translocation of ATP7B from the SAC to the bile canaliculus after removal of BFA.

in the SAC suggests that the same mechanisms of transport that operate in the SAC could function in both the transcytosis of ATP7B and in its apical recycling.

The inhibition of apical ATP7B endocytosis by DYN is consistent with the bile canaliculus being the site of ATP7B function in Cu^+ excretion. It should be noted that this finding confirms previous observations of Cu^+-induced translocation of ATP7B from the TGN to the bile canaliculus in HepG2 cells and the localization of ATP7B in the bile canaliculus of liver (Guo et al., 2005; Roelofsen et al., 2000; Schaefer et al., 1999b), and that these studies have been subsequently confirmed in other cells by other laboratories (Guo et al., 2005; Hernandez et al., 2008).

It is intriguing to note that although most of the membrane proteins resident in the bile canaliculus that contain multiple transmembrane-spanning sequences are directly targeted from the Golgi (Kipp and Arias, 2002), ATP7B in contrast uses a distinct transcytosis route to reach the bile canaliculus, a route that was previously thought to be restricted to apical proteins with a single transmembrane domain (Bastaki et al., 2002).

The conclusions of the studies reported here are in contrast with those of a recent study in HepG2 cells that proposes that ATP7B is rapidly and directly targeted from the TGN to lysosomes in response to Cu^+ and that fusion of the Cu^+-loaded lysosomes with the bile canaliculus membrane results in the excretion of excess Cu^+ into the bile (Polishchuk et al., 2014). The latter studies extend previous reports that interpret the presence and functioning of transfected GFP–ATP7B and ATP7B–DsRed constructs in late endosomes as part of the lysosome-mediated excretion of Cu^+ into the bile. In those studies, the ATP7B constructs were not detected in the TGN and were not relocated in response to excess Cu^+ (Harada et al., 2005, 2003b, 2000a,b). In contrast, in our studies in highly polarized Can 10 cells, we observe that excess Cu^+ induces the rapid translocation of endogenous ATP7B from the TGN to the bile canaliculus by basolateral sorting and transcytosis. Moreover, during this rapid trafficking process, we did not find any association of ATP7B with lysosomes and, repeating these studies using HepG2 cells, we could not find any ATP7B in the lysosomes in response to treatment with Cu^+ in these cells. Furthermore, we did not observe any Cu^+-induced movement of lysosomes towards the bile

Journal of Cell Science (2016) 129, 2190-2201 doi:10.1242/jcs.184663

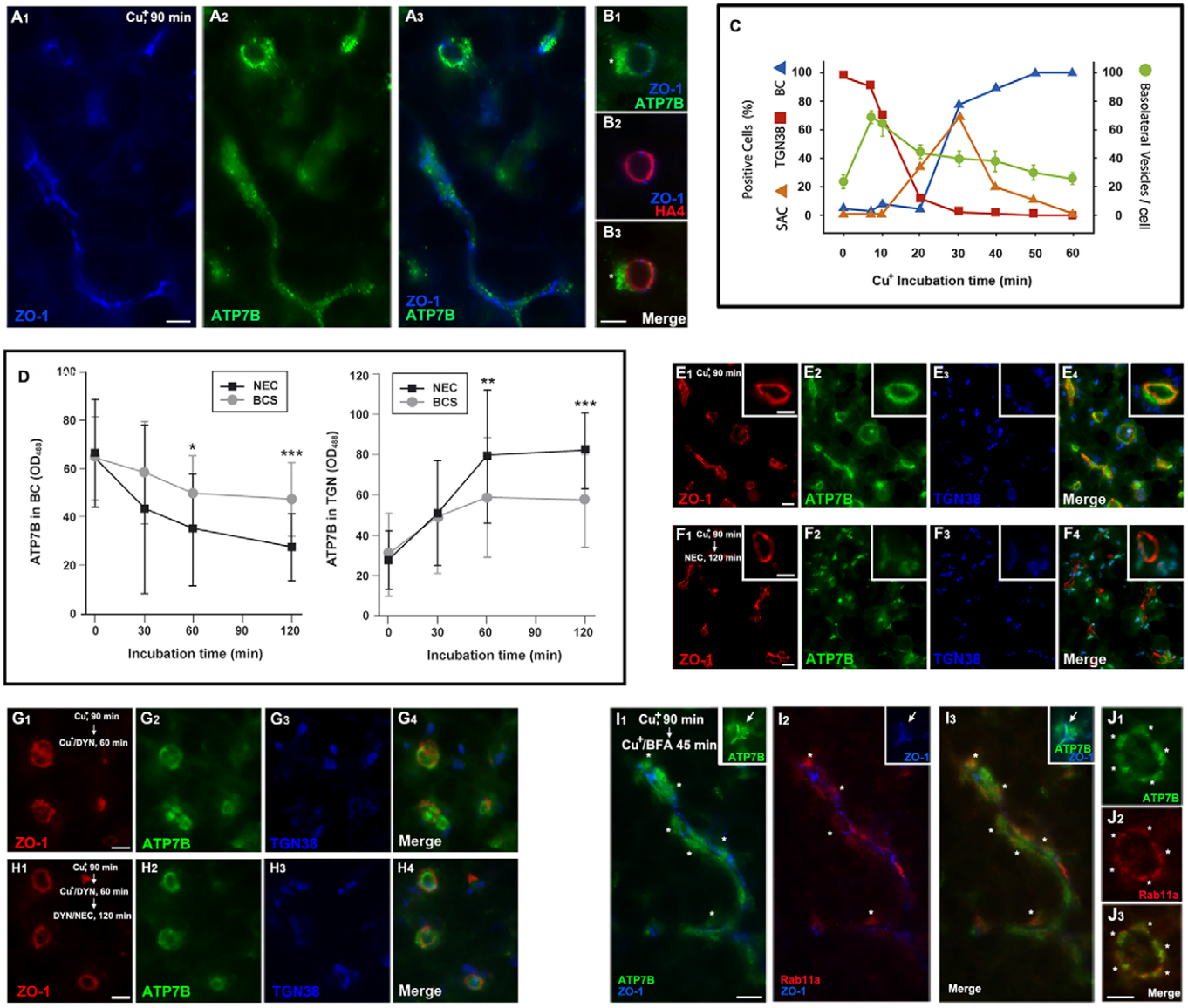

Fig. 7. ATP7B incorporation into the bile canaliculus, DYN-sensitive apical endocytosis and BFA-sensitive apical recycling. ATP7B incorporation into the bile canaliculus was studied in cells with long and short bile canaliculi that had been treated for 90 min with 40 µM Cu^+, and stained for ATP7B and ZO-1 (A1–A3) and the bile canaliculus membrane marker HA4 (B1–B3). Notice the retention of ATP7B in the bile canaliculus that is boxed and sealed by the ZO-1-positive tight junctions, and the co-localization of ATP7B with the apical membrane marker HA4; ATP7B-loaded apical endosomes are marked with an asterisk. Time course of the Cu^+-dependent ATP7B relocation from the TGN to the bile canaliculus. Cells were fixed and permeabilized after incubation with 40 µM Cu^+ for the indicated times were stained for ATP7B, TGN38, Rab11aA and HA4 (C); single organelles (TGN, SAC, bile canaliculus) and basolateral vesicles were counted in 50 cells per time point [(median±winsorized standard deviation (Sw0.2)]. The experiment shown is representative of three experiments. ATP7B apical endocytosis and retrograde transport to the TGN. Cells that had been preincubated for 90 min with Cu^+ were incubated after washing out Cu^+ with 100 µM of the cell-permeable and impermeable Cu^+-chelating agents NEC and BCS, respectively, for the times indicated (D); notice that the action of NEC was strongest. Incubation with NEC induced the complete translocation of ATP7B to the TGN after 120 min of incubation (D; compare E and F). *P<0.05, **P<0.01, ***P<0.001 (Student's t-test). ATP7B apical recycling and retrograde transport. Apical ATP7B endocytosis was studied in Can 10 cells that had been incubated for 90 min with 40 µM Cu^+ and then for 60 min with 80 µM DYN and Cu^+ (G1–G4), before removal of Cu^+ and incubation for 2 h with DYN and 100 µM NEC (H1–H4); treatment showed the strong inhibition of ATP7B apical endocytosis by the dynamin inhibitor DYN. Apical recycling of endocytosed ATP7B. Recycling was studied in cells that had been incubated for 90 min with 40 µM Cu^+ and then for a further 45 min with 10 µg/ml BFA in the presence of Cu^+; compare panels I1–J3 with panels A1–B3 and notice the retention of ATP7B in the RAb11a-positive SAC, flanking the tight junctions, of the BFA-treated cells. Arrows in the inset of I indicate the association of a pool of ATP7B with the tight junctions, and asterisks in I indicate the SAC. Scale bars: 10 µm.

canaliculus, nor did we detect any incorporation of four distinct LIMPs into the bile canaliculus, as would be expected if the excretion of Cu^+ was primarily mediated by lysosomal exocytosis.

The picture emerging from studies in human and frozen sections of rat liver is that endogenous ATP7B is localized in the TGN and in the bile canaliculus (Schaefer et al., 1999a,b). However, more studies are needed to establish the response of the ATP7B that is retained in the TGN to excess Cu^+ in liver.

It is important that abnormal intracellular trafficking of the Cu^+ transporters has been detected in multisystemic diseases that present with symptoms like those of Menkes and Wilson diseases. The transport of ATP7B from the TGN to the bile canaliculus through basolateral sorting and transcytosis explains that two of those

Journal of Cell Science (2016) 129, 2190-2201 doi:10.1242/jcs.184663

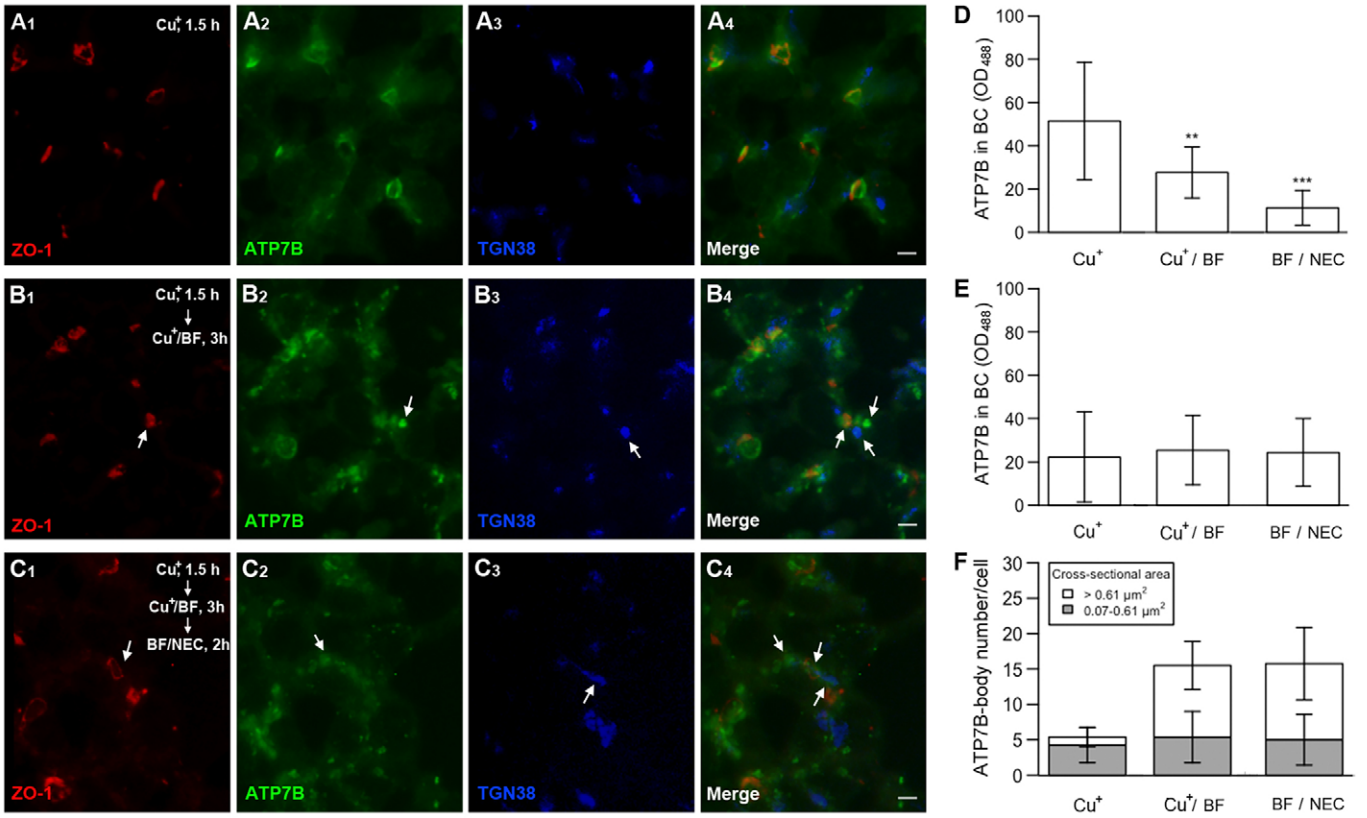

Fig. 8. Bafilomycin A1 blocks ATP7B apical recycling and retrograde transport to the TGN. Can 10 cells that had been first incubated for 90 min with 40 µM Cu^+ to induce the translocation of ATP7B to the bile canaliculus (A1–A4) were then incubated for 3 h with 60 nM bafilomycin A1 and Cu^+ (B1–B4) and, after washing out of Cu^+, were incubated for 2 h with bafilomycin A1 and 100 µM NEC (C1–C4). The cells that had been treated with bafilomycin A1 in the presence of Cu^+ showed the accumulation of ATP7B in vesicular bodies that were distinct from bile canaliculus and TGN (compare A and B, arrows), and bafilomycin A1 (BF) blocked the retrograde transport of ATP7B to the TGN after removal of Cu^+ through NEC treatment (C1, arrows). The intensity of fluorescence of ATP7B in the bile canaliculus (D) and TGN (E), and size of ATP7B-positive vesicular bodies (F) were quantified. Data collected from 20 bile canaliculi and 50 TGN in three randomly selected fields (mean±s.d.); $^{**}P<0.01$, $^{***}P<0.001$ (Student's *t*-test). Scale bars: 5 µm.

multisystemic diseases are produced by mutations that target AP-1A (Martinelli et al., 2013), the clathrin adaptor resident in the TGN that is implicated in the basolateral sorting of protein in the hepatocyte (Gravotta et al., 2012), and COMMD1 (van De Sluis et al., 2002), the component of the CCC complex that in cooperation with the WASH complex and the retromer regulates the trafficking of cargo through basolateral endosomes in polarized cells and is required for transcytosis (Phillips-Krawczak et al., 2015; Verges et al., 2004). These observations emphasize the importance of elucidating the mechanisms that regulate the trafficking of Cu^+ transporters in order to facilitate diagnoses, and to understand the development and prognosis of Cu^+ disorders.

In closing, this study describes that the Cu^+-dependent relocation of ATP7B from the TGN to the bile canaliculus includes basolateral sorting at the TGN, and transport to and endocytic retrieval at the basolateral membrane, which is followed by microtubule-dependent transcytosis through the SAC and incorporation into the bile canaliculus. These results indicate that the site of ATP7B action in vectorial Cu^+ excretion is the membrane of the bile canaliculus.

MATERIALS AND METHODS

Cell culture

Rat hepatoma Can 10 and human hepatoma HepG2 cells were grown in Coon's modification medium supplemented with 1.5 g/l $NaCO_3H$, 10% fetal calf serum, 1% glutamax, penicillin and streptomycin. Can 10 cells were cultured for 5 days for complete surface polarization, and medium was changed daily. Counting of basolateral vesicles was facilitated by growing the Can 10 cells on poly-lysine-coated coverslips and incubating the cells for 10 h in Coon's medium supplemented with 0.5 mM 3-isobutyl-1-methylxanthine.

cDNA cloning, constructs and transfections

Mouse ATP7B cDNA was cloned by PCR amplification of a mouse liver Marathon Ready cDNA library (Lalioti et al., 2014). Exofacial HA-tagging of ATP7B was performed by introducing the tag into the third exofacial loop of ATP7B (Lalioti et al., 2014). Cells were transfected for 11 h using Lipofectamine 2000 to avoid protein overexpression and incubated with 50 µg/ml cycloheximide for the final 3 h to inhibit new ATP7B synthesis.

Antibodies

Polyclonal anti-ATP7B antibodies were developed in rabbit and rat against the entire N-terminal cytoplasmic domain of the protein (Hernandez et al., 2008). The following antibodies were also developed in our laboratory: Mouse monoclonal and rabbit polyclonal antibodies against TGN38 (Yuan et al., 1987), rabbit polyclonal anti-LAMP2 antibody and mouse monoclonal antibodies against lysosomal integral membrane proteins CD63 (LIMP1), LIMPII and LAMP1 (LIMPIII) (Barriocanal et al., 1986), and rabbit polyclonal against LAMP2. Monoclonal antibodies against the apical marker HA4 (c19) and the tight junction protein ZO-1 (R26.4C) were developed by Drs A. Hubbard (Johns Hopkins University, MD) and D. A. Goodenough (Harvard Medical School, MA), respectively, and were obtained from the Developmental Studies Hybridoma Bank, created by the NICHD of the NIH and maintained at The University of Iowa, Department of Biology, Iowa City, IA 52242. Other antibodies used were: mouse monoclonal anti-HA clone 16B12 (Covance, CA; catalogue number MMS-101P); mouse IgG1 anti-β catenin and anti-EEA1 (BD Biosciences,

Journal of Cell Science (2016) 129, 2190-2201 doi:10.1242/jcs.184663

catalogue numbers 610154 and 610546); mouse monoclonal anti-Rab 11a (Abcam, UK; cat. 78337); rat monoclonal YOL 1/34 anti-tubulin (Sigma Aldrich, MO; catalogue number CBL270): Goat anti-α adaptin (Santa Cruz Biotech.; catalogue number 6422). Specific antibodies were used at 1:600 and 1:1000 dilutions in immunofluorescence microscopy and western blotting studies, respectively Alexa-Fluor-488-, Alexa-Fluor-647- and Pacific-Blue-conjugated secondary antibodies and Alexa-Fluor-647-conjugated transferrin were from Life Technologies.

Chemicals

Neocuproine (NEC), bathocuprine disulfonate (BCS) and brefeldin A (BFA) were from Sigma-Aldrich; nocodazole (NOC) and dynasore (DYN) and chloroquine (CQ) were from Santa Cruz Biotech; Bafilomycin A1 was from Shelleckchem.

Immunofluorescence microscopy

Cell fixation was adapted to antibody reactivity; fixation and permeabilization was performed by treatment with cold (−20°C) methanol for 4 min [for antibodies against ATP7B, ZO-1, YOL 1/34 (tubulin), TGN38, β-catenin, CD63, LIMPII, LAMP1 and LAMP2], for 20 min with 2% paraformaldehyde and 5 min with 0.2% Triton X-100 [for antibodies against ATP7B, ZO-1, Rab11a, YOL 1/34 (tubulin), HA tag and EEA1] or for 1 min with 3% paraformaldehyde and 10 min with methanol at 5°C (for antibodies against ATP7B, ZO-1, HA4). All antibodies were diluted 1:300 in PBS containing 0.2% bovine serum albumin.). For colocalization studies, cells were grown on 0.1–0.16-mm glass coverslips and mounted in gelvatol (refractive index 1.376). Stable Alexa-Fluor-488 and Alexa-Fluor-647 dyes were used to avoid spectral bleed, and the stained cells were examined using a Zeiss Plan apochromat ×63 NA1.4 oil DIC objective and oil with a refractive index of 1.51. Capture Images were de-convoluted and studied using Coloc 2 and JACoP modules of ImageJ software. Data were subjected to robust statistical analyses.

ATP7B trafficking assays

The de-acidification agent bafilomycin A1, the dynamin inhibitor DYN, the microtubule inhibitor NOC, the ARF-GEF inhibitor BFA and incubation at low temperature were used to treat cells and help dissect the pathway of transport. Translocation of ATP7B from the TGN to the bile canaliculus was studied by challenging Can 10 cells with 40 µM Cu^+ for periods between 5 min and 2 h; the translocation process was best monitored in small islets of highly polarized cells. The effective retention of ATP7B in the TGN at 0.3 µM Cu^+ made unnecessary the use of Cu^+-chelating agents to start protein trafficking of ATP/B with most of it in the TGN. In a set of trafficking experiments, we established as landmarks of the ATP7B anterograde traffic, the beginning (5–7 min) and completion (10–20 min) of its release from the Golgi, its appearance in basolateral endosomes loaded with endocytosed transferrin (8–20 min), its approach and entrance into the SAC (15–35 min), and its incorporation into the bile canaliculus (30 min–1 h) (see Fig. 7C). These landmarks helped to set a series of traps to dissect the pathway of ATP7B transport: bafilomycin A1 and chloroquine were employed to slow down the release of ATP7B by acidic vesicles from the TGN; DYN, the inhibitor of dynamin and clathrin-dependent endocytosis, was used at 80 µM in serum-free medium to examine the trafficking of ATP7B through the basolateral membrane; NOC, the microtubule-depolymerizing agent, was a powerful tool to study the second leg of trafficking between the basolateral membrane and the SAC, and the incorporation of ATP7B into the bile canaliculus; we incubated cells for 15 min with Cu^+ to target ATP7B from the TGN to basolateral endosomes, and then for 1 h with Cu^+, NOC and BFA at 4°C to disrupt the microtubules and to set the stage to study the redistribution of basolateral ATP7B after warming the cells in the absence of NOC, and the presence or absence of BFA; the trapping of ATP7B in the SAC of cells that had been warmed in the absence of NOC and in the presence of BFA helped to characterize the passage of ATP7B through the SAC and indicated the involvement of a BFA-sensitive ARF-GEF in the regulation of ATP7B targeting from the SAC to the bile canaliculus, probably apical BIG2; for studies of apical ATP7B endocytosis and retrograde transport, the cell permeable agent NEC was the Cu^+-chelating agent of choice because it quickly elicits the backwards trafficking of ATP7B in response to decreased Cu^+ levels, the cell-impermeable agent BCS was less effective; DYN was a powerful tool to study the apical endocytosis of ATP7B in cells that had been deprived of Cu^+ through treatment with NEC, whereas BFA was effective in trapping the apically endocytosed ATP7B in cells that had been continuously incubated with Cu^+. The experiments were repeated an average of three times.

Immunoprecipitation and western blot studies

All the procedures were performed at 4°C. Can 10 cells were washed twice with TBS, scraped, suspended in 1 ml of cold buffer A [20 mM HEPES pH 7.5, 130 mM NaCl, 1 mM EGTA and 5.5 mg of the cocktail of protease inhibitors Complete Mini (Roche)] and incubated in 1% NP40 for 10 min. Nuclei were removed by centrifugation at 100 ***g*** for 10 min. The resulting post-nuclear supernatant was incubated at 4°C for 1 h, aggregates were removed by centrifugation at 15,000 ***g*** for 10 min, and the supernatant was diluted using buffer A to a final concentration of 0.6% NP40. Equal aliquots of extract were separately incubated for 4 h with the rabbit anti-ATP7B antibody (dilution 1:300 in PBS containing 0.2% bovine serum albumin) or the goat anti-AP-2α antibody (dilution 1:300 in PBS containing 0.2% bovine serum albumin.) bound to Protein-G–Sepharose, prepared by mixing 5 µl of each antibody with 15 µl of Protein-G–Sepharose (GE Healthcare) and then washing off excess antibody. Immunoprecipitation complexes were collected by low-speed centrifugation and, after three washes in buffer A and one in water, were resuspended and heated (85°C, 3 min) in Laemmli buffer and resolved by performing 10% SDS-PAGE. The resolved proteins were blotted onto nitrocellulose and studied using bioluminescence, donkey anti-rabbit horseradish peroxidase (HRP)-conjugated (GE Healthcare) and donkey anti-goat HRP-conjugated (Merck Millipore) antibodies, and the Clean Blot IP detection kit (Thermo Scientific). The ATP7B–AP-2α pulldown experiment was repeated twice.

Acknowledgements

We thank Dr Camilo Colaco for useful suggestions, Dr Carlos García for help with the LIMP sequencing and José Belio for help with the artwork.

Competing interests

The authors declare no competing or financial interests.

Author contributions

V.L. and I.V.S. planned and performed cell biology and biochemical experiments, antibody development and manuscript writing; R.P. performed statistical analysis and edited the manuscript; M.P.-B. performed ATP7B apical endocytosis and retrograde transport assays and edited the manuscript. Y.T. performed the ATP7B anterograde transport assay and antibody development; A.M. and T.V. performed confocal microscopy, deconvolution and image analysis. C.S. performed conventional and confocal microscopy and wrote the manuscript.

Funding

This work was supported by grants from the Instituto de Salud Carlos III [grant number PI11/00922]; the Fundació per Amor a L'Art (2014); and the Fundación Areces (2013). M.P.-B. was supported by a fellowship from Consejo Superior de Investigaciones Científicas.

Supplementary information

Supplementary information available online at
http://jcs.biologists.org/lookup/suppl/doi:10.1242/jcs.184663/-/DC1

References

Barriocanal, J. G., Bonifacino, J. S., Yuan, L. and Sandoval, I. V. (1986). Biosynthesis, glycosylation, movement through the Golgi system, and transport to lysosomes by an N-linked carbohydrate-independent mechanism of three lysosomal integral membrane proteins. *J. Biol. Chem.* **261**, 16755-16763.

Bastaki, M., Braiterman, L. T., Johns, D. C., Chen, Y.-H. and Hubbard, A. L. (2002). Absence of direct delivery for single transmembrane apical proteins or their "Secretory" forms in polarized hepatic cells. *Mol. Biol. Cell* **13**, 225-237.

Braiterman, L., Nyasae, L., Guo, Y., Bustos, R., Lutsenko, S. and Hubbard, A. (2009). Apical targeting and Golgi retention signals reside within a 9-amino acid sequence in the copper-ATPase, ATP7B. *Am. J. Physiol. Gastrointest. Liver Physiol.* **296**, G433-G444.

Braiterman, L., Nyasae, L., Leves, F. and Hubbard, A. L. (2011). Critical roles for the COOH terminus of the Cu-ATPase ATP7B in protein stability, trans-Golgi network retention, copper sensing, and retrograde trafficking. *Am. J. Physiol. Gastrointest. Liver Physiol.* **301**, G69-G81.

Bull, P. C., Thomas, G. R., Rommens, J. M., Forbes, J. R. and Cox, D. W. (1993). The Wilson disease gene is a putative copper transporting P-type ATPase similar to the Menkes gene. *Nat. Genet.* **5**, 327-337.

Cassio, D., Macias, R. I. R., Grosse, B., Marin, J. J. G. and Monte, M. J. (2007). Expression, localization, and inducibility by bile acids of hepatobiliary transporters in the new polarized rat hepatic cell lines, Can 3–1 and Can 10. *Cell Tissue Res.* **330**, 447-460.

Cox, R., Mason-Gamer, R. J., Jackson, C. L. and Segev, N. (2004). Phylogenetic analysis of Sec7-domain-containing Arf nucleotide exchangers. *Mol. Biol. Cell* **15**, 1487-1505.

de Hoop, M., von Poser, C., Lange, C., Ikonen, E., Hunziker, W. and Dotti, C. G. (1995). Intracellular routing of wild-type and mutated polymeric immunoglobulin receptor in hippocampal neurons in culture. *J. Cell Biol.* **130**, 1447-1459.

Donoso, M., Cancino, J., Lee, J., van Kerkhof, P., Retamal, C., Bu, G., Gonzalez, A., Caceres, A. and Marzolo, M.-P. (2009). Polarized traffic of LRP1 involves AP1B and SNX17 operating on Y-dependent sorting motifs in different pathways. *Mol. Biol. Cell* **20**, 481-497.

Gravotta, D., Carvajal-Gonzalez, J. M., Mattera, R., Deborde, S., Banfelder, J. R., Bonifacino, J. S. and Rodriguez-Boulan, E. (2012). The clathrin adaptor AP-1A mediates basolateral polarity. *Dev. Cell* **22**, 811-823.

Guo, Y., Nyasae, L., Braiterman, L. T. and Hubbard, A. L. (2005). NH2-terminal signals in ATP7B Cu-ATPase mediate its Cu-dependent anterograde traffic in polarized hepatic cells. *Am. J. Physiol. Gastrointest. Liver Physiol.* **289**, G904-G916.

Harada, M., Sakisaka, S., Kawaguchi, T., Kimura, R., Taniguchi, E., Koga, H., Hanada, S., Baba, S., Furuta, K., Kumashiro, R. et al. (2000a). Copper does not alter the intracellular distribution of ATP7B, a copper-transporting ATPase. *Biochem. Biophys. Res. Commun.* **275**, 871-876.

Harada, M., Sakisaka, S., Terada, K., Kimura, R., Kawaguchi, T., Koga, H., Taniguchi, E., Sasatomi, K., Miura, N., Suganuma, T. et al. (2000b). Role of ATP7B in biliary copper excretion in a human hepatoma cell line and normal rat hepatocytes. *Gastroenterology* **118**, 921-928.

Harada, M., Kawaguchi, T., Kumemura, H. and Sata, M. (2003a). Where is the site that ATP7B transports copper within hepatocytes? *Gastroenterology* **125**, 1911; author reply 1911-2.

Harada, M., Kumemura, H., Sakisaka, S., Shishido, S., Taniguchi, E., Kawaguchi, T., Hanada, S., Koga, H., Kumashiro, R., Ueno, T. et al. (2003b). Wilson disease protein ATP7B is localized in the late endosomes in a polarized human hepatocyte cell line. *Int. J. Mol. Med.* **11**, 293-298.

Harada, M., Kawaguchi, T., Kumemura, H., Terada, K., Ninomiya, H., Taniguchi, E., Hanada, S., Baba, S., Maeyama, M., Koga, H. et al. (2005). The Wilson disease protein ATP7B resides in the late endosomes with Rab7 and the Niemann-Pick C1 protein. *Am. J. Pathol.* **166**, 499-510.

Harris, E. D. (2000). Cellular copper transport and metabolism. *Annu. Rev. Nutr.* **20**, 291-310.

Hernandez, S., Tsuchiya, Y., García-Ruiz, J. P., Lalioti, V., Nielsen, S., Cassio, D. and Sandoval, I. V. (2008). ATP7B copper-regulated traffic and association with the tight junctions: copper excretion into the bile. *Gastroenterology* **134**, 1215-1223.

Hoekstra, D., Tyteca, D. and van IJzendoorn, S. C. D. (2004). The subapical compartment: a traffic center in membrane polarity development. *J. Cell Sci.* **117**, 2183-2192.

Holloway, Z. G., Velayos-Baeza, A., Howell, G. J., Levecque, C., Ponnambalam, S., Sztul, E. and Monaco, A. P. (2013). Trafficking of the Menkes copper transporter ATP7A is regulated by clathrin-, AP-2-, AP-1-, and Rab22-dependent steps. *Mol. Biol. Cell.* **24**, 1735-1748, S1-8.

Hunziker, W., Male, P. and Mellman, I. (1990). Differential microtubule requirements for transcytosis in MDCK cells. *EMBO J.* **9**, 3515-3525.

Jain, S., Farias, G. G. and Bonifacino, J. S. (2015). Polarized sorting of the copper transporter ATP7B in neurons mediated by recognition of a dileucine signal by AP-1. *Mol. Biol. Cell* **26**, 218-228.

Kenney, S. M. and Cox, D. W. (2007). Sequence variation database for the Wilson disease copper transporter, ATP7B. *Hum. Mutat.* **28**, 1171-1177.

Kipp, H. and Arias, I. M. (2002). Trafficking of canalicular ABC transporters in hepatocytes. *Annu. Rev. Physiol.* **64**, 595-608.

Lalioti, V., Muruais, G., Tsuchiya, Y., Pulido, D. and Sandoval, I. V. (2009). Molecular mechanisms of copper homeostasis. *Front. Biosci.* **14**, 4878-4903.

Lalioti, V., Hernandez-Tiedra, S. and Sandoval, I. V. (2014). DKWSLLL, a versatile DXXXLL-type signal with distinct roles in the Cu(+)-regulated trafficking of ATP7B. *Traffic* **15**, 839-860.

Martinelli, D., Travaglini, L., Drouin, C. A., Ceballos-Picot, I., Rizza, T., Bertini, E., Carrozzo, R., Petrini, S., de Lonlay, P., El Hachem, M. et al. (2013). MEDNIK syndrome: a novel defect of copper metabolism treatable by zinc acetate therapy. *Brain* **136**, 872-881.

Metzelaar, M. J., Schuurman, H.-J., Heijnen, H. F. G., Sixma, J. J. and Nieuwenhuis, H. K. (1992). Biochemical and immunohistochemical characteristics of CD62 and CD63 monoclonal antibodies. Expression of GMP-140 and LIMP-CD63 (CD63 antigen) in human lymphoid tissues. *Virchows Arch. B Cell Pathol. Incl. Mol. Pathol.* **61**, 269-277.

Nyasae, L. K., Schell, M. J. and Hubbard, A. L. (2014). Copper directs ATP7B to the apical domain of hepatic cells via basolateral endosomes. *Traffic* **15**, 1344-1365.

Phillips-Krawczak, C. A., Singla, A., Starokadomskyy, P., Deng, Z., Osborne, D. G., Li, H., Dick, C. J., Gomez, T. S., Koenecke, M., Zhang, J.-S. et al. (2015). COMMD1 is linked to the WASH complex and regulates endosomal trafficking of the copper transporter ATP7A. *Mol. Biol. Cell* **26**, 91-103.

Polishchuk, E. V., Concilli, M., Iacobacci, S., Chesi, G., Pastore, N., Piccolo, P., Paladino, S., Baldantoni, D., van IJzendoorn, S. C. D., Chan, J. et al. (2014). Wilson disease protein ATP7B utilizes lysosomal exocytosis to maintain copper homeostasis. *Dev. Cell* **29**, 686-700.

Roelofsen, H., Wolters, H., Van Luyn, M. J. A., Miura, N., Kuipers, F. and Vonk, R. J. (2000). Copper-induced apical trafficking of ATP7B in polarized hepatoma cells provides a mechanism for biliary copper excretion. *Gastroenterology* **119**, 782-793.

Schaefer, M., Hopkins, R. G., Failla, M. L. and Gitlin, J. D. (1999a). Hepatocyte-specific localization and copper-dependent trafficking of the Wilson's disease protein in the liver. *Am. J. Physiol.* **276**, G639-G646.

Schaefer, M., Roelofsen, H., Wolters, H., Hofmann, W. J., Müller, M., Kuipers, F., Stremmel, W. and Vonk, R. J. (1999b). Localization of the Wilson's disease protein in human liver. *Gastroenterology* **117**, 1380-1385.

Tanzi, R. E., Petrukhin, K., Chernov, I., Pellequer, J. L., Wasco, W., Ross, B., Romano, D. M., Parano, E., Pavone, L., Brzustowicz, L. M. et al. (1993). The Wilson disease gene is a copper transporting ATPase with homology to the Menkes disease gene. *Nat. Genet.* **5**, 344-350.

Uemura, T., Suda, Y., Ueda, T. and Nakano, A. (2014). Dynamic behavior of the trans-golgi network in root tissues of Arabidopsis revealed by super-resolution live imaging. *Plant Cell Physiol.* **55**, 694-703.

van de Sluis, B., Rothuizen, J., Pearson, P. L., van Oost, B. A. and Wijmenga, C. (2002). Identification of a new copper metabolism gene by positional cloning in a purebred dog population. *Hum. Mol. Genet.* **11**, 165-173.

Vergés, M., Luton, F., Gruber, C., Tiemann, F., Reinders, L. G., Huang, L., Burlingame, A. L., Haft, C. R. and Mostov, K. E. (2004). The mammalian retromer regulates transcytosis of the polymeric immunoglobulin receptor. *Nat. Cell Biol.* **6**, 763-769.

Weiss, K. H., Lozoya, J. C., Tuma, S., Gotthardt, D., Reichert, J., Ehehalt, R., Stremmel, W. and Füllekrug, J. (2008). Copper-induced translocation of the Wilson disease protein ATP7B independent of Murr1/COMMD1 and Rab7. *Am. J. Pathol.* **173**, 1783-1794.

Welz, T., Wellbourne-Wood, J. and Kerkhoff, E. (2014). Orchestration of cell surface proteins by Rab11. *Trends Cell Biol.* **24**, 407-415.

Yilla, M., Tan, A., Ito, K., Miwa, K. and Ploegh, H. L. (1993). Involvement of the vacuolar H(+)-ATPases in the secretory pathway of HepG2 cells. *J. Biol. Chem.* **268**, 19092-19100.

Yuan, L., Barriocanal, J. G., Bonifacino, J. S. and Sandoval, I. V. (1987). Two integral membrane proteins located in the cis-middle and trans-part of the Golgi system acquire sialylated N-linked carbohydrates and display different turnovers and sensitivity to cAMP-dependent phosphorylation. *J. Cell Biol.* **105**, 215-227.